Water Research 179 (2020) 115876

Contents lists available at ScienceDirect

Water Research

journal homepage: www.elsevier.com/locate/watres

Insights into catalytic removal and separation of attached metals from natural-aged microplastics by magnetic biochar activating oxidation process

Shujing Ye [a], Min Cheng [a], Guangming Zeng [a, *], Xiaofei Tan [a, **], Haipeng Wu [a, b, ***], Jie Liang [a], Maocai Shen [a], Biao Song [a], Jiaqi Liu [a], Hailan Yang [a], Yafei Zhang [a]

[a] College of Environmental Science and Engineering, Hunan University and Key Laboratory of Environmental Biology and Pollution Control (Hunan University), Ministry of Education, Changsha, 410082, PR China
[b] School of Hydraulic Engineering, Changsha University of Science & Technology, Changsha, 410114, PR China

ARTICLE INFO

Article history:
Received 18 November 2019
Received in revised form
21 April 2020
Accepted 22 April 2020
Available online 28 April 2020

Keywords:
Natural-aged microplastics
Attached Pb
Organic matter
Biochar
SR-AOPs

ABSTRACT

Natural-aged microplastics with changed surface properties accumulate, redistribute and spread in all water fields as carriers of hazardous substances. The combined hazard of co-contamination of microplastics and hazardous substances expands the ecological risks, which urgently needs to design treatment schemes for pollutant removal from microplastics. In this paper, a facile and applicable magnetic biochar with porosity and graphitization (PGMB) was prepared for realizing the goal of metal removal from the microplastics. Heterogeneous catalysis of persulfate (PS) activated by PGMB achieved the decomposition of organics, with the decrease of more than 60% of the attached Pb on the surface of microplastics, and the adsorbed metal amount by PGMB in this system (31.29 mg/g) is much higher than that by the individual PGMB group (7.07 mg/g). Analysis demonstrated that the organic layer covered on the microplastic surface over the long-term weathering provided the key sites for metal sorption, whose decomposition and peeling were the critical steps in whole process. The prepared PGMB was responsible for activating PS to produce reactive species for decomposing the organic matter accompanied with detaching metals from microplastic surface, also would keep the role for re-adsorption of the released metals and separation from aqueous phase by magnetic force. The influences of natural environmental factors including salinity, common matrix species, and temperature on the performance of PGMB/PS system for metal removal from microplastics were discussed to illustrate the universality of the scheme in saline or organic-rich waters. The results of this study provided underlying insights for removing metals from microplastic surface, and decreasing the harm risks in the co-contamination of microplastics and hazardous substances.

1. Introduction

The prevalence, distribution and influence of plastic particles in the natural environment have received considerable attention of scientists and government managers. The annual production amount of waste plastics had been reported to surpass 348 million tons (Shen et al., 2019a), and these various plastics are released into aquatic environment through irresponsible handling, illegal dumping and aquaculture activities. Processes of fragmentation and embrittlement would occur on the discarded plastics when they are exposed to solar radiation, temperature change, physical effects of wind currents and waves, as well as the biological effects (Fotopoulou and Karapanagioti, 2015; Shen et al., 2019c). The fragmented plastic particles whose diameter is smaller than 5 mm are defined as microplastics, which become the focus of research owing to their potential toxic risk in aquatic ecosystem and human health (Farrell and Nelson, 2013; Tanaka et al., 2013). Because of the small dimension that similar to the ingested food and the

* Corresponding author.
** Corresponding author.
*** Corresponding author.College of Environmental Science and Engineering, Hunan University and Key Laboratory of Environmental Biology and Pollution Control (Hunan University), Ministry of Education, Changsha, 410082, PR China.
E-mail addresses: zgming@hnu.edu.cn (G. Zeng), tanxf@hnu.edu.cn (X. Tan), wuhaipeng@csust.edu.cn (H. Wu).

https://doi.org/10.1016/j.watres.2020.115876
0043-1354/

ubiquitous distribution whether suspended or deposited, microplastics are regarded as a huge threat to aquatic organisms through inadvertent ingestion, entanglement and smothering. The hard-digestible microplastics can block the esophagus, but also lead to a false sense of fullness (Mrosovsky et al., 2009; Taylor et al., 2016; Wright et al., 2013). Besides the physical harms of microplastics, a related concern is the attachment and enrichment of hazardous substances onto the surface of microplastics causing chemical toxicity. As a result, microplastics act as a component of the suspended load shown precise role for long-range transport of contaminants (Holmes et al., 2014; Huffer and Hofmann, 2016; Shen et al., 2019b). Many researches have indicated that microplastics could act as vectors to increase metals and organic chemicals exposure in organisms (Hodson et al., 2017; Koelmans et al., 2016; Massos and Turner, 2017). Furthermore, the microplastics along with the adsorbed hazardous substances can not only raise the risk of inflammation and immune impairment on organisms (Carbery et al., 2018), but also be capable of promoting the bioaccumulation and biomagnification of hazardous contaminants via the food chain.

Considerable research efforts have been devoted to the adsorption behaviors of hazardous substances onto different types of microplastics (Huffer and Hofmann, 2016; Wu et al., 2019; Xu et al., 2018) that depended on both the microplastic types and pollutant properties. Due to the wide distribution of microplastics likely to be exposed to heavy metals and organic pollutants in natural environment, microplastics exhibit substantial potential on adsorption of harmful substances. The properties of microplastic such as polarity, specific surface area, degree of crystalline structure, and abundance of rubbery (Brennecke et al., 2016) show significant impacts on adsorption behavior of persistent organic pollutants through hydrophobic interactions, electrostatic forces, H-binding and noncovalent bonds (Wu et al., 2019; Zhang et al., 2018a). Attaching charged metal ions onto inherently neutral surface of plastics seems to be infeasible, since the microplastic surface has no inherent characteristics for extra attraction to metal ions. However, the natural-aged microplastics suspended in aqueous environment with loss of physical integrity for a long-term basis can gain charges and a larger surface area by surface modification of biofilm formation, weathering, and attrition or precipitation of inorganic minerals. These surface changes endow aged microplastics with accessibility to hazardous substance, and metal adsorption was found to be considerably greater to aged microplastics than to virgin microplastics (Holmes et al., 2014; Kalcikova et al., 2020). Studies confirmed that pollutant adsorption on microplastic surface was improved in the presence of organic matter especially the humic acid than fulvic acid, which was resulted from the π-π conjugation between humic acid and microplastic that provided a suitable and charged surface for attraction and adsorption of various pollutants (Zhang et al., 2018a). Although the health effects of ingesting microplastics alone have not been formally established, higher toxic effects on aquatic life had been verified due to the combined toxic function of hazardous substances and microplastics (Dong et al., 2019; Turner and Holmes, 2015). Research confirmed that aged microplastics with biofouling was tested for adsorbing silver at environmentally relevant concentrations, and showed more adsorbed amount and intensive subsequent leaching of silver. The following toxicological experiments proved that aged microplastics attached with silver had high ecotoxicological potential on daphnids *Daphnia magna*, yet little toxicity could be found by pristine microplastics (Kalcikova et al., 2020). Surprisingly, little attention has been committed to remove the attached hazardous substances from microplastics for decreasing the risk of co-contamination. On the basis of the above views, it can be concluded that the organic matter layer (biofilm) formed naturally over time on the microplastic surface endows the microplastic surface with the ability to adsorb metals through bridging role. In order to achieve the purpose of removing heavy metals from microplastics, the decomposition and exfoliation of the organic layer adhering to the microplastic surface is crucial.

Microplastics exposed to the aquatic environment are gradually coated by a layer of inorganic and organic substances, which provides available surface for the colonization of microorganisms to inhabit followed by forming biofilm (Oberbeckmann et al., 2015; Rummel et al., 2017; Zhang et al., 2018b). The subsequent formation of conditioning layer containing microorganisms (live or dead) and the embedded extracellular polymeric substance (EPS) shows great potential for metal adsorption. For transforming the organic layer that bears the bridging role, advanced oxidation processes especially the sulfate radical-based one (SR-AOPs) has hopeful prospects in decomposing organic matter by in-situ generated reactive species (Liu et al., 2019; Luo et al., 2019; Oh et al., 2016; Tang et al., 2018; Yi et al., 2019). Heterogeneous catalysis for SR-AOPs is of great interest to many researchers, in which the selection and preparation of catalysts are the focus of research (Gong et al., 2009; Wang et al., 2019a; Xu et al., 2012). Biochar-based material with high graphitization is increasingly reported as a promising redox-active catalyst to mineralize organics into carbon dioxide and water by the active sites of defects and versatile functional groups (Chen et al., 2018; Oh et al., 2018; Wang et al., 2019b; Zhang et al., 2019). Besides the carbon matrix, biochar with appropriate pore structure can be used as a carrier to support transition metals and their oxides which configured with variable valence to coordinate the activation process of persulfate (PS) (Fu et al., 2019; Yu et al., 2019). Fe is considered as a better alternative of transition metals, not only because of its wide range of sources and hypotoxicity, more importantly, attributed to its inherent magnetism which provides a beneficial opportunity to achieve material recycling (Yu et al., 2019). In addition to the function of catalyst, the performance of biochar as adsorbent to immobilize metal ions had been intensively investigated (Ye et al., 2017a; Zeng et al., 2019; Zhang et al., 2013). Owing to the abundant functional groups and large cation exchange capacity (Song et al., 2019a; Xiong et al., 2018), biochar exhibits considerable adsorption capacity for metal ions, therefore provides a powerful platform for re-immobilizing metals that are detached from the microplastic surface and reduces the mobile form of metal.

This paper first proposed the view of removing metals from microplastics by decomposing the organic matter layer covered on the surface, in order to alleviate the potential harms of microplastics as vectors to transport hazardous substances and reduce the co-contamination. Considering the additional chemical toxicity of heavy metals attached to aged-microplastics, sulfate radical-based AOPs were regarded as novel and cost-effective technology to remove heavy metals from the surface of the microplastic, as well as separating the released heavy metals from the water simultaneously by magnetic catalyst. Lead (Pb), a frequently detected heavy metal in aquatic environment, is treated as a representative target pollutant. In this study, a highly efficient biochar-based catalyst containing ferromagnetic property was prepared by modification of K_2FeO_4 (a green and multi-functional water treatment agent playing the role to improve pore formation and graphitization). The performance of prepared biochar-based catalyst to activate persulfate for decomposition of organic matter covered on microplastic surface and to achieve immobilization and recovery of the released metal ions was explored. The main research purposes are to (1) explore the decomposition of the organic matter layer through SR-AOPs, in which PS is activated by biochar-based catalyst; (2) determine the content change of metal

on the microplastic surface during the experiment; (3) discuss the effects of coexisting substances (inorganics and organics) in actual water, salinity and temperature on the performance of PGMB/PS system for metal removal from microplastics; and (4) analyze the main treatment mechanisms involved in degradation of organics, separation of attached metal from microplastics, and re-adsorption of released metal.

2. Materials and methods

2.1. Materials

Natural-aged (beached) plastics were sampled from bottomland of Dongting Lake, a wetland located in Hunan Province, China. In the laboratory, the sand on the plastic surface was carefully removed by soaking in ultrapure water, and then the dried samples pass through a 20-mesh sieve to ensure that the particle dimensions fall into the range of microplastics definition. Standard Lead reserve solution, potassium ferrate (K_2FeO_4), sodium persulfate ($Na_2S_2O_8$, PS) were purchased from Shanghai Chemical Corp. Besides, all used solutions were prepared in high purity ultrapure water (18.25 MΩ cm) which was produced by Ulupure (UPRII-10 T) laboratory water system.

2.2. Synthesis of biochar-based catalyst

Straw collected from shallow flats of Dongting Lake was washed and shattered to a particle size of <0.15 mm as precursor. Then, the straw powders were immersed in 100 mL aqueous solution of K_2FeO_4 (0.1 M) with continuous stirring lasting for 12 h. Undergone vacuum drying at 80 °C overnight, the acquired solid was transferred into a quartz boat and annealed in tube furnace at a temperature of 900 °C for a residence time of 2 h at continuous flow of N_2 gas. The carbonized black solid after naturally cooling with porous structure, improved graphitization as well as magnetism was denoted as PGMB.

2.3. Characterization methods

The surface morphological and structural differences between virgin and aged microplastics were characterized via field emission scanning electron microscope (SEM, QUANTA Q400, USA). Surface functional groups of microplastics in different states were qualitatively detected by fourier transform infrared spectrum (FTIR, Nicolet 5700 Spectrometer) recorded in the range of 4000−400 cm^{-1}. The zeta potentials analysis used to determine the surface charge of microplastics was performed by Electroacoustic Spectrometer (ZEN3600 Zetasizer, UK). EDX elemental mapping was used to discover the variation of Pb on microplastic surface before and after adsorption equilibrium, as well as undergone treatment of SR-AOPs.

In addition, the surface properties of the prepared biochar were also characterized. X-ray photoelectron spectroscopy (XPS, ESCALAB 250Xi, USA) with the calibration of C1s at 284.8 eV was applied to test the chemical states of element under an Al-Kα X-ray radiation. The pore characteristics of biochar-based catalyst were calculated by automatic surface-area porosity analyzer (Quantachrome Instrum Quadrasorb EVO, USA) on the basis of N_2 isotherms at 77.3 K.

2.4. Treatment experiments

Microplastics (MPs) that had been pre-wetted were poured into 250 mL conical flask containing 100 mL solution of Pb at a concentration of 10 mg/L. Moderate shaking was carried out in a thermostatic shaker to establish the adsorption-desorption equilibrium over night (pre-experiment confirmed that the equilibrium state was reached at 6 h). The adsorption capacity was calculated by $q_t = (C_0\text{-}C_t)*V/m$ (C_0 (mg/L): initial Pb concentration in solution; C_t (mg/L): residual Pb concentration at t; V (mL): reaction solution volume; m (mg): the mass of the microplastic) and taken as the amount of Pb that adhered onto the microplastic surface prior to the SR-AOPs treatment. In a typical treatment process, 15 mg of the synthesized biochar was suspended in above solution, followed by adding a certain amount of $Na_2S_2O_8$ (maintaining final solution containing 0.25 mM PS) to trigger the oxidation reaction. The solution samples were withdrawn at each time interval and used for determination of parameters in solution after filtration by 0.45 μm PVDF disposable filters. After 4 h of experiments, the attached metal onto the microplastic surface were extracted by digestion with acid and measured by atomic absorption spectrometry (PEAA700, USA), and the attached content of Pb on microplastics was calculated by $q_m = C_1{*}V_0/m_1$ (C_1 (mg/L): Pb concentration in digestion solution; V_0 (mL): volume of digestion liquid; m_1 (mg): the mass of the microplastic involved in digestion). The differences in metal amount of MPs before experiment, and Fe leaching from PGBC after reaction were detected through coupled plasma mass spectrometry (ICP-MS, Agilent 7800). The transformation of organic matter in solution across the treatment was measured by three-dimensional excitation and emission matrix fluorescence spectroscopy (3D EMMs) recorded on FluoroMax-4 fluorescence spectrophotometer.

3. Results and discussion

3.1. Characterization

First of all, it could be visually distinguished between natural-aged and virgin MPs on the basis of their external surface color (Fig. S1). The darker color was assigned to the aged MPs resulted from the attachment of organisms, such as algaes, mosses, microbes and their secretions on the microplastic surface. More detailed differences in surface morphology of microplastics can be observed by SEM images (Fig. 1). Virgin microplastics were in the uniform shape of fragments with smooth and flat surface (Fig. 1b), since they were derived from the artificially mechanical fragmentation of commercial plastics. Notably, the natural-aged MPs displayed changes in the morphology, roughness and chemical properties on surface compared with virgin ones. The surface of aged MPs was rougher and presented macroscopic networks of microcracks with covering protrusions and deposition owing to chain scission of the polymer and mineral adhesion, showing the characteristics of porous polymer. Table S1 shows the differences of metal content between virgin and natural-aged microplastics determined by ICP-MS under the same digestion condition. It can intuitively demonstrate that the metals such as Mg, Al, Mn and Fe, related to mineral deposition, are much more abundant in weathered microplastics than in the virgin ones. The huge difference in Cd content could be explained by the fact that Cd was accumulated over a long period on natural-aged microplastics which were collected from shallow flats of Dongting Lake where was polluted by Cd. The wrinkled and aggregated structure of aged MPs might result in larger specific surface area and more potential adsorption sites for metal capture, which also could reveal the affinity of microplastics for different organisms and their tendency for surface biofouling.

The surface functional groups of microplastics before and after weathering were characterized by FTIR and shown in Fig. 1c. Variations in absorption peak position and peak intensity can be observed between them. Different from the spectrum of virgin

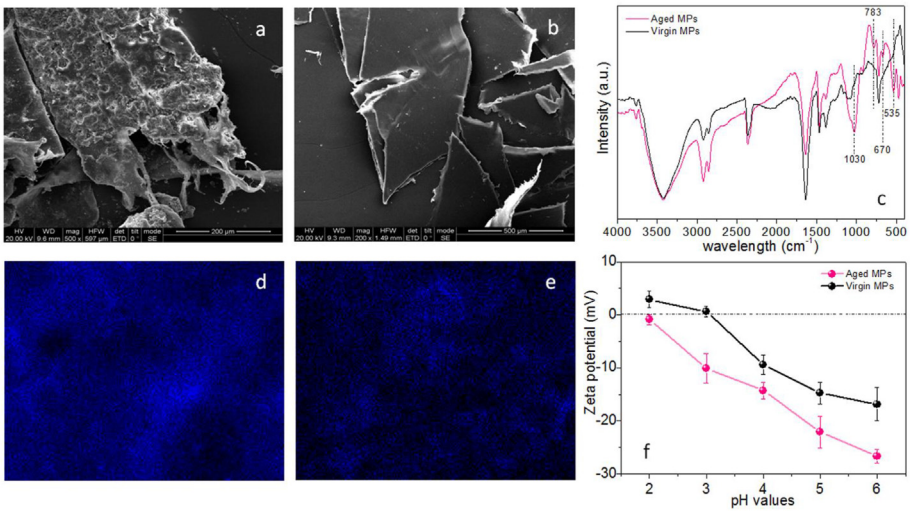

Fig. 1. SEM images of natural-aged (a) and virgin microplastic surface (b); FTIR spectrums of natural-aged and virgin MPs (c); Pb elements on aged MPs before (d) and after (e) SR-AOPs in PGMB/PS system by EDS mapping analysis; and Zeta potentials of natural-aged and virgin MPs at different pH ranging from 2.0 to 6.0 (f).

microplastic, a broadened new peak located at ~1030 cm^{-1} was detected on the aged microplastic, which is attributed to the C—O—C stretching vibration of ester. In addition, the new bands appearing at peak position of 535, and 785 cm^{-1} are assigned to the in-plane bending vibration of the C═O in aliphatic ketone and the oscillations of C—O of hetero-aromatic ring, respectively. These variations in oxidation peaks of aged MPs are derived from the long-term photo-oxidation by reaction with atmospheric oxygen during light irradiation assisted with biodeterioration, when plastic was exposed to the natural environment (Fotopoulou and Karapanagioti, 2015; Zhu et al., 2019). Besides the hetero-aromatic ring structure which was not found in the virgin MPs, the peak positioned at ~670 cm^{-1} in spectrum of aged microplastic could be derived from the C—P vibration of phosphorus-containing compounds, which may be a proof for the organics covering on the surface of natural-aged microplastic.

The Zeta potentials of aged and virgin suspended microplastics under different pH values were investigated, which reflected the surface charges. According to the results obtained by Fig. 1f, the negative values of both MPs in a near-neutral pH manifested microplastics could be stabilized and minimally aggregated in the natural aquatic environments, owing to interparticle electrostatic repulsion (Li et al., 2018). The surface of aged microplastics showed electronegative on a pH range of 2—6 and decreased gradually with increasing pH value. Compared with the virgin MPs, the aged MPs accumulated more negative charges on surface, and the zero point of charge (pH_{zpc}) drop from 3.06 examined by virgin MPs suspension to less than 2.00 by aged MPs suspension, which was accounted for the changes in physico-chemical properties of aged microplastic surface or the adhesion of negatively charged organic matter and minerals onto the surface in natural environment for long time.

3.2. PS/PGBC performance for metal removal from microplastic surface

Surface modification of aged MPs was formed by long-term weathering, UV-induced photo-oxidation, high temperature and humidity, and typical conditions encountered at beaches. These variations endow microplastic with larger specific surface area, porosity and oxygen-containing functional groups, as well as turning charge through biofilm formation and mineral precipitation (Holmes et al., 2014; Turner and Holmes, 2015). The more heterogeneous and reactive surface induces greater adsorption capacity of aged MPs than that of the virgin ones by electrostatic interactions, cation exchange and co-precipitation. Fig. S2 shows a time-dependent adsorption process and kinetics curve of Pb by natural-aged MPs, whose saturated adsorption capacity can reach as high as 20.15 mg/g, confirming the strong adsorption performance of aged MPs and the role in respect of the transport and behavior of metals in aquatic environment. Compared with the equilibrium adsorbed amount of Pb by virgin microplastics calculated to be 4.63 mg/g under the same surrounding conditions, it could be further clarified that the organic layer as well as the deposited minerals on MP surface formed by weathering was of great importance for metal accumulation.

The Pb content attached to the microplastic surface was calculated to be 19.83 mg/g measured by the acid digestion method, which was very close to the adsorbed amount calculated by the Pb concentration in solution at the equilibrium of adsorption (20.15 mg/g). Therefore, it is convincing that the content of Pb attached onto the microplastic surface before SR-AOPs treatment was calculated by equilibrium adsorption with Pb concentration in the solution at the subsequent experiments. Undergone adsorption-desorption equilibrium within 24 h, samples were exposed to different treatment of individual PGMB, PS, and SR-AOPs treatment with PS activated by PGMB lasting for 4 h. As shown in Fig. 2a, compared with the negligible Pb removal from microplastic surface under non-treatment, treatment by PGMB, and PS alone, successful combination system of PGMB and PS is likely to inspire the removal improvement for attached Pb on microplastic surface with an over 60% removal efficiency (calculated by the ratio of Pb content on MPs after SR-AOPs treatment to the Pb content on MPs after adsorption). To identify the changes in Pb on microplastic surfaces, elemental mapping analysis under scanning transmission electron microscopy (STEM) mode was carried out to characterize the element distribution. The evident contrast differences of Pb distribution on microplastic surfaces before and after oxidation treatment by PGMB/PS system could be observed on Fig. 1. This was a strong evidence for Pb distribution with large amount on the surface of microplastics after adsorption operation (Fig. 1d), while the signal of the attached Pb was significantly reduced after the SR-AOPs reaction by PGMB/PS system (Fig. 1e).

It is worthwhile mentioning that the adsorbed amount of Pb on

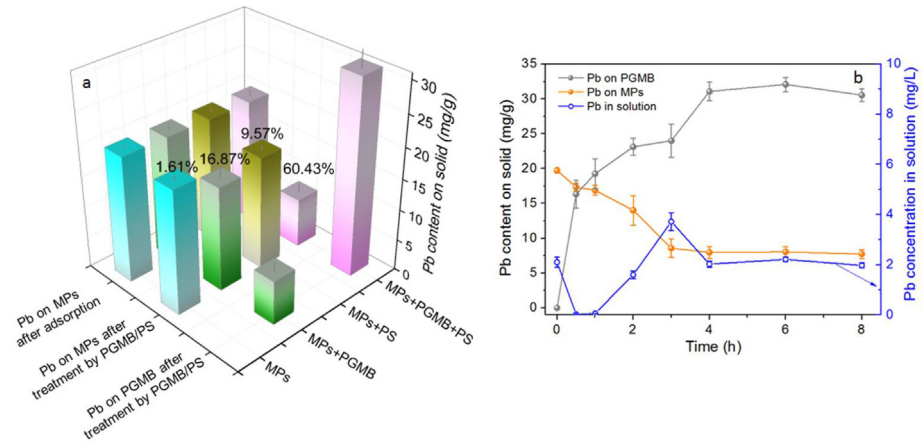

Fig. 2. Pb content on solid (MPs and PGMB) at each stage in different treatment groups.

biochar surface was observed to increase significantly from 7.07 mg/g at treatment of PGMB individual to 31.29 mg/g at PGMB/PS treatment, which not only proved that the prepared biochar has excellent adsorption properties for metals, but also indirectly verified the advanced oxidation process of PS activated by PGMB would help the attached Pb to fall off from the microplastic surface and thereby provide more opportunities for metal removal. To gain more insight, we explored the variation of Pb concentration in different parts (MPs, PGMB, and solution) with different periods, as shown in Fig. 2b. It could be found that once the AOPs were triggered by adding biochar into vessels, PGMB can rapidly adsorb metal in the solution while activate PS to destroy the organic matter covered on microplastic surface for the Pb detachment from surface. The fluctuating Pb concentration in solution reflected the process of Pb desorption from microplastic surface and re-adsorption onto PGMB. Until the end of the reaction, the Pb concentration in the solution changed little compared with that before AOPs treatment, reflecting that the concentration of mobile Pb would not be increased, which indicated that the ecological risk of Pb in the solution could be effectively controlled. As the contact time increased, the attached content of Pb on microplastics surface gradually decreased, while the adsorbed amount of Pb on PGMB significantly increased, realizing the transfer of metal from microplastic to biochar surface and achieving the purpose of metal separation through magnetic force (Scheme 1).

Concerning the potential vehicle role of microplastics for transfer of chemicals from river to ocean, the influences of various factors in the natural environment on the performance of PGMB/PS system for metal removal need to be further discussed. The performance of the PGMB/PS system from adsorption to separation removal of metal on microplastic surface under different salinity gradients is shown in Fig. 3a. A distinct decrease of the attached Pb on microplastic surface could be found within the NaCl electrolyte, which may be explained by the competition of sodium ion for occupying the adsorption site, and shielding negative charge of the microplastic surface to reduce electrostatic attraction. Although the final attached content of Pb was lower in the salinity group than in the control, the metal removal efficiency from the microplastic surface slightly decreased with the increase of salinity, due to its low basic adsorption. NaCl exhibited an inhibitory effect on the detachment of Pb from the microplastic surface, as Cl^- can be served as radical scavenger (Yang et al., 2018; Zhou et al., 2019) to produce less reactive chlorine radical that adversely affected the exfoliation and breaking of organic layers. Another possible explanation is that the microplastic particles tend to be agglomerated at a higher salinity, which is determined by the less electrostatic repulsion and the steric effect with compression of the electrical double layer (Li et al., 2018; Turner and Holmes, 2015), reducing the opportunities of contact between the microplastic surface and the reactive species generated on the surface of biochar, followed by a decrease in degradation toward organic matter on MP surface.

In order to deeply investigate the practical application, several common matrix species were discussed systematically for their effects on metal removal by PGMB/PS system. Fig. 3b displays the different attached amount of Pb on solid (MPs and PGMB) as well as the metal removal efficiency in the presence of various (in)organics. The pH buffering action of HCO_3^- and HPO2− 4 resulted from hydrolysis can alkalinize the solution to a certain extent, where an alkaline environment would benefit the precipitation or complexation of Pb and reduce the amount of available Pb(II) for adsorption in solution. In terms of the metal removal from microplastic surface based on the radical oxidation, there is no denying that HCO_3^- and HPO_4^{2-} have great potential as scavenger to immediately capture radicals (Song et al., 2019b; Ye et al., 2019a), thereby inhibiting the decomposition of organic matter and removal of metal on surface. The difference between the two groups of HCO_3^- and HPO_4^{2-} is the adsorbed amount of Pb on PGMB at the end of treatment. It may arise from the fact that the biochar surface is still attractive for adsorption or adhesion of metals or their precipitation generated in the HCO_3^- group, while the metals in HPO_4^{2-} group tended to generate soluble complexes by chelating effect. A decreasing tendency in the attached amount of Pb on MPs surface was found as the humic acid (HA) content increased, which was attributed to the extra interaction of HA as organic ligands with metals to produce (in)soluble complex compounds with stable chemical properties. It should be mentioned that there seems to be no significant effect of added amount of HA with regard to the metal removal from microplastic surface. It indicated that HA is more likely to affect the metal chelated affinity partition, and influence limitedly the oxidation performance of reactive species generated by PGMB/PS system.

Considering that microplastics have experienced numerous seasonal cycles in nature, the effects of ambient temperature on metal removal from microplastic surface by PGMB/PS system were further explored. On the basis of the results in Fig. S3, it can be concluded that higher temperature showed slight inhibited effect on Pb adsorption to microplastic surface. Two possible explanations are responsible for this phenomenon: (1) high temperature favors the thermal motion of molecules in solution, thereby enhancing the

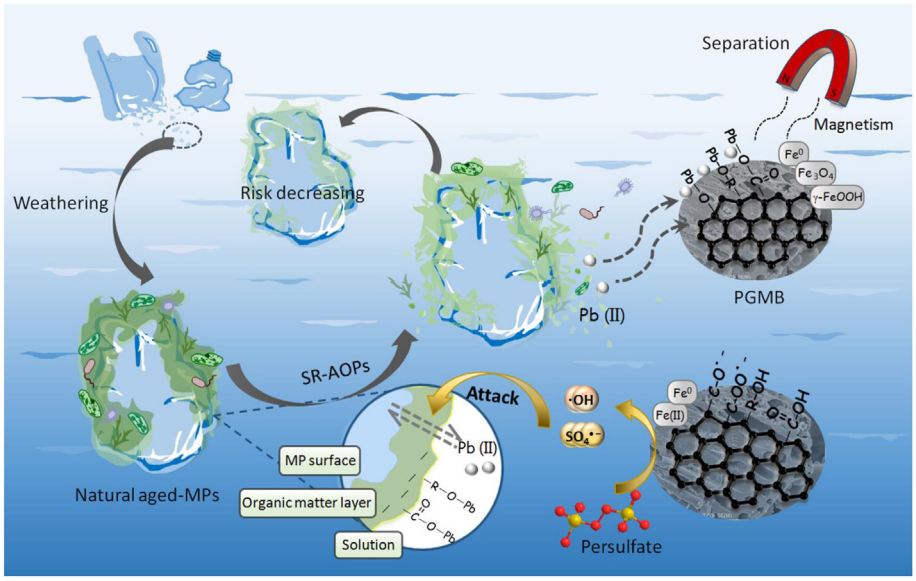

Scheme 1. Proposed mechanism of SR-AOPs performance by PGMB/PS system for organics degradation and metal detachment from natural-aged microplastic surface.

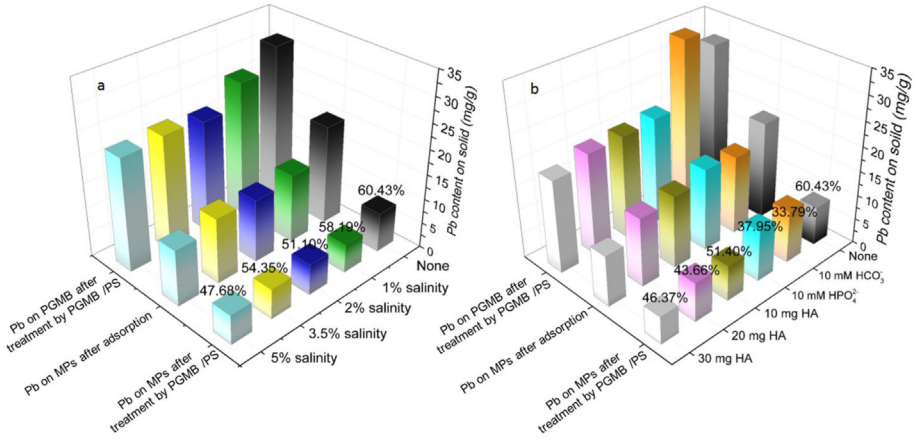

Fig. 3. Effect of salinity (a); and common matrix species (b) on Pb content and metal removal efficiency from MP surface by PGMB/PS system.

Pb(II) mobility; (2) metal attachment on microplastics dominated by physical interaction is a reversible process, where the temperature rise is more conducive to the occurrence of desorption reaction. In addition, temperature is observed to have a remarkable impact on metal removal behavior from microplastic surface. More radical generation by PS decomposition at higher temperature could account for the larger removal efficiency of metal, as more radicals were involved in decomposing the organic matter that attached onto the microplastic surface. Based on the observation on Fig. S3, Pb adsorption by PGMB is a spontaneous, endothermic process dominated by chemical interaction, indicating warming is likely to inspire more metal recovery with high adsorbed amount on biochar surface.

3.3. Mechanism exploration

The surface properties of the prepared PGMB were characterized to gain more insight into its ability to activate PS decomposition and adsorb metal. As can be seen from Fig. 4a, a plenty of hollow tubes consisted of thin-walled carbon with rough surface was observed by SEM, on which many small bumps were assigned to be iron-containing particles. The uneven surface and the abundant pores on it provide a platform for the occurrence of various reactions. The BET specific surface area of PGMB was calculated to be about 76.316 m^2/g testing by N_2 isotherms at 77K. A IV-type isothermal curve with a large hysteresisloop demonstrated the characteristic of mesoporous, where the average pore size was detected to be 3.732 nm based on pore size distribution by the BJH model. Appropriate specific surface area and pore size distribution improved the surface accessibility for drawing PS melocules and metals to trigger surface reaction. The graphitic structure and crystallinity of the prepared PGMB were provided by XRD patterns (Fig. 4b). A diffraction peak appearing at 26.5° was ascribed to the (002) plane of graphite, demonstrating the locally ordered carbon structure even with the introduction of iron. Three typical characteristic peaks corresponding to Fe^0 were found at 2θ values of 44.6°, 65.2° and 82.3° in XRD spectrum, respectively, indicating that Fe^0 is the most important form of iron in the prepared biochar. Fe^0 had been intensively investigated to exhibit strong activation ability for PS decomposition due to its low valence state, it can not only produce more radicals by the heterogeneous transportation of electrons from Fe^0 to PS, but also continuously and slowly provide

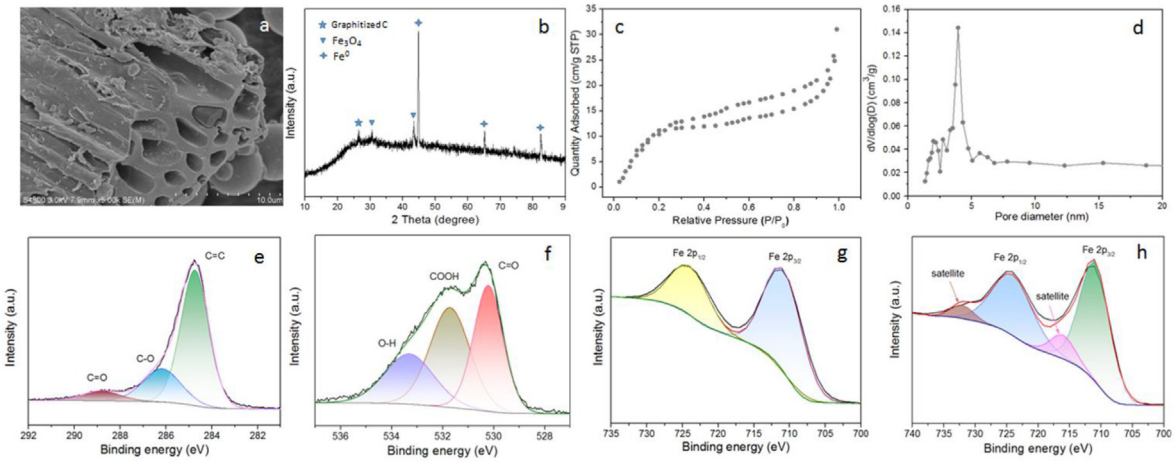

Fig. 4. SEM image (a), XRD pattern (b), N_2 adsorption-desorption isotherm (c), pore-size distribution curve (d) of the prepared PGMB, the high resolution XPS spectrum of C 1s (e), O 1s (f); Fe 2p before (g) and after AOPs treatment (h) in PGMB.

Fe(II) for radical generation (Eqs. (1)–(3)), avoiding the quenching reactions between Fe(II) ion and $SO_4^{\bullet}$–(Oh et al., 2010; Peluffo et al., 2016). The other two weak peaks locating at 30.5° and 43.3° were indexed to the (220), and (400) crystal planes of Fe_3O_4, further confirming the ferromagnetism of PGMB which allows metal could be separated from aqueous phase. The VSM magnetization curve (Fig. S4) of the recovered PGMB was examined with saturation magnetization value of 55.51 emu/g for verifying the magnetic properties of PGMB after the whole treatment. X-ray photoelectron spectroscopy was performed to analyze the valence state of each element in PGMB. There are three fitted peaks in high-resolution spectrum of C1s shown in Fig. 4e, positioned at 284.8, 286.2, and 288.8 eV, corresponding to C═C bonds in aromatic ring, C–O (alkoxy), and ketonic C═O, respectively, in which carbonyl and ketone groups had been proved to be the active site for triggering advanced oxidation processes (Duan et al., 2016; Shao et al., 2018; Ye et al., 2020). Moreover, most of the oxygen-containing functional groups, such as C═O (ketonic group), COOH (carboxyl), and H–O located at 530.2, 531.7, and 533.3 eV, respectively, detected in the O1s high-resolution spectrum were regarded as sites for metal adsorption (Tan et al., 2015; Ye et al., 2017b, 2019b). Fig. 4g and h displays the binding energies of Fe 2p peaks at 710.9, and 724.1 eV referring to the $2p_{3/2}$ and $2p_{1/2}$ orbit of Fe, respectively. The additional satellite peaks of PGMB appeared in the high-resolution spectrum of Fe 2p after the AOPs reaction suggested the increase in oxidation state Fe(Ⅲ), which was due to the participation of low valence Fe in PS activation with Fe cycle (Eqs. (3)–(7)).

$$\equiv Fe^0 + H_2O \rightarrow \equiv Fe(II) + OH^- + H_2 \quad (1)$$

$$\equiv Fe^0 + O_2 + 2H_2O \rightarrow 2 \equiv Fe(II) + 4\ OH^- \quad (2)$$

$$\equiv Fe^0 + 2\ S_2O_8^{2-} \rightarrow 2 \equiv Fe(II) + 2\ SO_4^{\bullet} - + 2\ SO_4^{2-} \quad (3)$$

$$\equiv Fe(II) + S_2O_8^{2-} \rightarrow \equiv Fe(III) + SO_4^{\bullet} - + SO_4^{2-} \quad (4)$$

$$\equiv Fe(III) + 2\ H_2O \rightarrow \equiv Fe(III)OOH + 3\ H^+ \quad (5)$$

$$2 \equiv Fe(III)OOH + 2\ SO_4^{2-} + 2\ H_2O \rightarrow 2 \equiv Fe(II)\ SO_4 + 4\ OH^- + H_2 + O_2 \quad (6)$$

$$\equiv Fe(III) + S_2O_8^{2-} \rightarrow \equiv Fe(II) + S_2O_8^{\bullet} - \quad (7)$$

$$\equiv C-OOH + S_2O_8^{2-} \rightarrow \equiv C-OO^{\bullet} - + SO_4^{\bullet} - + HSO_4^- \quad (8)$$

$$\equiv C-OH + S_2O_8^{2-} \rightarrow \equiv C-O^{\bullet} - + SO_4^{\bullet} - + HSO_4^- \quad (9)$$

$$\equiv Quinones + H_2O \rightarrow 2 \equiv Semiquinone^{\bullet -} + 2H^+ \quad (10)$$

$$\equiv Semiquinone^{\bullet -} + S_2O_8^{2-} \rightarrow SO_4^{\bullet} - + \equiv Quinones \quad (11)$$

To shed light on the role of the organic layer covering the surface on metal attachment by microplastics, we deeply studied the relationship between the decomposition degree of organic matter on microplastic surface by acid or alkali treatment with the adsorbed amount of Pb on the surface, thus illustrating the feasibility of separating metals from microplastic surface through the decomposition of organic matter covering on it. Considering the different solubility of organic matter under the condition of acid and alkali, the aged-microplastics were shaken in different solutions to obtain various contents of organic matter coated on microplastics (different TOC values in aqueous phase). The pretreated microplastics were dried and used to explore their ability of metal adsorption. As shown in Fig. S5, it should be pointed out that the microplastic with the least amount of remaining organic matter on surface, reflected by the largest TOC value after the treatment of alkali liquor, resulted in the smallest metal adsorption capacity. The values of TOC in the pretreatment solution were inversely proportional to the amount of metal adsorbed on the microplastic surface (Fig. S5b), which proved that the decomposition of organic matter on the microplastic surface can achieve metal detachment and removal from microplastics.

In order to further confirm the decomposition and mineralization of the organic matter, 3D EMM spectra was carried out to identify the transformation and evolution of organic matter in solution across the oxidation process by PGMB/PS system. A sample of the solution, oscillated for 24 h with adding the same amount of microplastic as above experiment, showed the multiple peaks before SR-AOPs reaction (Fig. 5a). Based on spectrum elucidation, there were mainly three kinds of fluorescent peak positioned at Ex/Em of: 1) 250–300/280–380 nm (peak A associated with microbial by-product-like substances including tryptophan and tyrosine), 250–290/400–500 nm (peak B associated with fulvic acid-like compounds), and 320–380/400–490 nm (peak C associated with humic acid-like compounds), respectively. When the sample was collected by the reaction time of 1 h (Fig. 5b), the fluorescence

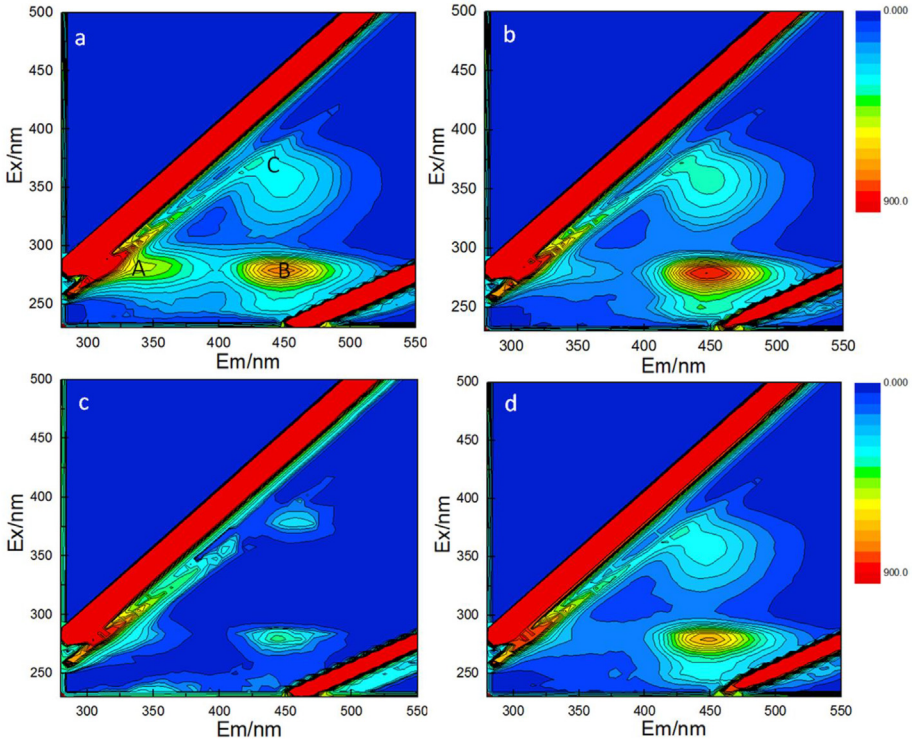

Fig. 5. 3D-EEM fluorescence spectroscopy of the water sample before SR-AOPs reaction (a); the sample undergone oxidation reaction by PGMB/PS system for 1 h (b), 2 h (c), and 4 h (d).

signal of the peak A that closely related to biology decreased markedly, which proved that this part of organic matter is most sensitive to the oxidation reaction by PGMB/PS system. Undergone 2 h of oxidation process, the intensity of the B and C peaks drop sharply even almost disappeared, describing that the fulvic acid-like and humic acid-like substances were decomposed by a large amount during this period, and they may be degraded into other intermediate products or mineralized thoroughly to produce CO_2 and H_2O. Extending the reaction time to 4 h (Fig. 5d), the fluorescence intensity of B and C peak abnormally increased dramatically, revealing that the organic substances originally covered onto the microplastic surface were destroyed and decomposed thereby released into solution. The FTIR spectrum of the microplastic that undergone the whole SR-AOPs was performed to analyze the transformation in surface properties in comparison with the microplastic before reaction (Fig. S6). The changes in either position or intensity of peaks associated with the covered organics on surface at 1420–1300 (carboxylate) and 900–600 cm^{-1} provided a supplementary explanation for the variation in coverage status of the organics on microplastic surface in the oxidation process.

The role of reactive species in the detachment of attached metals from microplastic surfaces and the types of active substances involved in the decomposition of organic matter can be analyzed by radical capture experiments. Methanol (MeOH) and tert-butyl-alcohol (TBA), at a molar ratio of 1000 to PS, were adopted as the scavengers of both sulfate and hydroxyl radicals, and

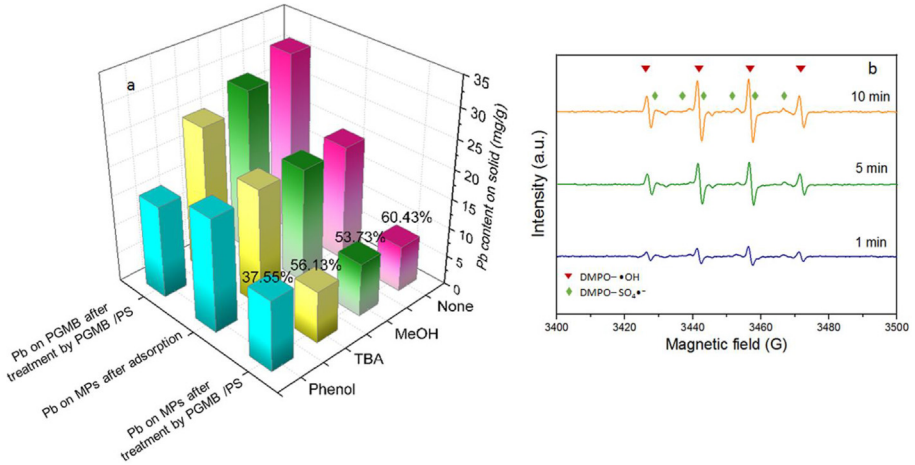

Fig. 6. Metal removal with additions of various scavengers (a); and EPR spectrum of species adducts trapped by DMPO in PGMB/PS system.

hydroxyl radicals, respectively, to consume the reactive species. The moderate degree of reduction in metal removal efficiency was provided on Fig. 6a, which preliminarily indicated that both $SO_4^{\bullet-}$and •OH were produced according to Eqs. (3)–(11), and participated in the metal removal process. Taking the hydrophilicity of scavengers but the radical generated on surface into account, the more hydrophobic scavenger for simultaneously capturing both radicals was applied. In the presence of phenol, the metal removal efficiency was found to be considerable decline from 60.45% to 37.55%, confirming the important role of radicals on metal detachment from microplastic surfaces. Electron paramagnetic resonance (EPR) spectrum with DMPO as spin trapping agents is a powerful evidence (Fig. 6b), in which the emergence of characteristic peaks of DMPO- $SO_4^{\bullet-}$and DMPO-•OH adducts directly illustrated the generation and revolution processes of reactive species on system. The metal removal by PGMB/PS system still proceeded even if the radicals were trapped, which was likely due to that the specific pathway of PS activation by carbon-based catalyst (non-radical degradation) continued to be a great impetus to organics decomposition (Luo et al., 2019; Zhu et al., 2018). The sharp decrease in the metal recovery by PGMB is owing to the fact that the coverage of hydrophobic substances on the surface restricts its adsorption site or accessible pathway, as well as less Pb detached from microplastic and released into solution.

4. Conclusions

In conclusion, the removal of the attached heavy metals from natural-aged microplastics was first achieved by the advanced oxidation reaction of PS activated by the prepared ferromagnetic biochar. The PGMB/PS system with reactive species generation and non-radical pathway was proposed to transform and decompose the covered organic matter (formed by long-term exposure to the environment) which acted the bridging role for metal adsorption on natural aged-microplastic surface. The metals that subsequently released from microplastic surface were re-immobilized by biochar with favorable specific surface area and abundant versatile functional groups, exhibiting great potential regarding the metal separation from aqueous phase through magnetic force. The anti-interference tests demonstrated that regardless of the differences in processing efficiency, the relatively less contents of metal were eventually remained on microplastic after reaction under various surrounding conditions. These new overall understandings provide novel opportunities for reducing the risks of microplastic pollution in water environments, especially the co-contamination of hazardous substances and microplastics.

Declaration of competing interest

The authors declare that they have no known competing financial interests or personal relationships that could have appeared to influence the work reported in this paper.

Acknowledgments

This research was financially supported by the National Natural Science Foundation of China (51521006, 81773333, 51809011, 51809089, and 51909084), the Program for Changjiang Scholars and Innovative Research Team in University (IRT-13R17), the Three Gorges Follow-up Research Project (2017HXXY-05), and the Science and Technology Plan Project of Hunan Province (No. 2019NK2062).

Appendix A. Supplementary data

Supplementary data to this article can be found online at https://doi.org/10.1016/j.watres.2020.115876.

References

Brennecke, D., Duarte, B., Paiva, F., Cacador, I., Canning-Clode, J., 2016. Microplastics as vector for heavy metal contamination from the marine environment. Estuar. Coast Shelf Sci. 178, 189–195.
Carbery, M., O'Connor, W., Palanisami, T., 2018. Trophic transfer of microplastics and mixed contaminants in the marine food web and implications for human health. Environ. Int. 115, 400–409.
Chen, X., Oh, W., Hu, Z., Sun, Y., Webster, R.D., Li, S., Lim, T., 2018. Enhancing sulfacetamide degradation by peroxymonosulfate activation with N-doped graphene produced through delicately-controlled nitrogen functionalization via tweaking thermal annealing processes. Appl. Catal. B Environ. 225, 243–257.
Dong, Y., Gao, M., Song, Z., Qiu, W., 2019. Adsorption mechanism of As(III) on polytetrafluoroethylene particles of different size. Environ. Pollut. 254 (Pt A), 112950.
Duan, X., Sun, H., Ao, Z., Zhou, L., Wang, G., Wang, S., 2016. Unveiling the active sites of graphene-catalyzed peroxymonosulfate activation. Carbon 107, 371–378.
Farrell, P., Nelson, K., 2013. Trophic level transfer of microplastic: Mytilus edulis (L.) to Carcinus maenas (L.). Environ. Pollut. 177, 1–3.
Fotopoulou, K.N., Karapanagioti, H.K., 2015. Surface properties of beached plastics. Environ. Sci. Pollut. Res. Int. 22 (14), 11022–11032.
Fu, Y.K., Qin, L., Huang, D.L., Zeng, G.M., Lai, C., Li, B.S., He, J.F., Yi, H., Zhang, M.M., Cheng, M., Wen, X.F., 2019. Chitosan functionalized activated coke for Au nanoparticles anchoring: green synthesis and catalytic activities in hydrogenation of nitrophenols and azo dyes. Appl. Catal. B Environ. 255, 117740.
Gong, J.L., Wang, B., Zeng, G.M., Yang, C.P., Niu, C.G., Niu, Q.Y., Zhou, W.J., Liang, Y., 2009. Removal of cationic dyes from aqueous solution using magnetic multi-wall carbon nanotube nanocomposite as adsorbent. J. Hazard Mater. 164 (2–3), 1517–1522.
Hodson, M.E., Duffus-Hodson, C.A., Clark, A., Prendergast-Miller, M.T., Thorpe, K.L., 2017. Plastic bag derived-microplastics as a vector for metal exposure in terrestrial invertebrates. Environ. Sci. Technol. 51 (8), 4714–4721.
Holmes, L.A., Turner, A., Thompson, R.C., 2014. Interactions between trace metals and plastic production pellets under estuarine conditions. Mar. Chem. 167, 25–32.
Huffer, T., Hofmann, T., 2016. Sorption of non-polar organic compounds by micro-sized plastic particles in aqueous solution. Environ. Pollut. 214, 194–201.
Kalcikova, G., Skalar, T., Marolt, G., Kokalj, A.J., 2020. An environmental concentration of aged microplastics with adsorbed silver significantly affects aquatic organisms. Water Res. 175 (2020), 115644.
Koelmans, A.A., Bakir, A., Burton, G.A., Janssen, C.R., 2016. Microplastic as a vector for chemicals in the aquatic environment: critical review and model-supported reinterpretation of empirical studies. Environ. Sci. Technol. 50 (7), 3315–3326.
Li, S., Liu, H., Gao, R., Abdurahman, A., Dai, J., Zeng, F., 2018. Aggregation kinetics of microplastics in aquatic environment: complex roles of electrolytes, pH, and natural organic matter. Environ. Pollut. 237, 126–132.
Liu, Y., Liu, Z., Huang, D., Cheng, M., Zeng, G., Lai, C., Zhang, C., Zhou, C., Wang, W., Jiang, D., Wang, H., Shao, B., 2019. Metal or metal-containing nanoparticle@MOF nanocomposites as a promising type of photocatalyst. Coord. Chem. Rev. 388, 63–78.
Luo, R., Li, M., Wang, C., Zhang, M., Nasir Khan, M.A., Sun, X., Shen, J., Han, W., Wang, L., Li, J., 2019. Singlet oxygen-dominated non-radical oxidation process for efficient degradation of bisphenol A under high salinity condition. Water Res. 148, 416–424.
Massos, A., Turner, A., 2017. Cadmium, lead and bromine in beached microplastics. Environ. Pollut. 227, 139–145.
Mrosovsky, N., Ryan, G.D., James, M.C., 2009. Leatherback turtles: the menace of plastic. Mar. Pollut. Bull. 58 (2), 287–289.
Oberbeckmann, S., Löder, M.G.J., Labrenz, M., 2015. Marine microplastic-associated biofilms – a review. Environ. Chem. 12 (5), 551.
Oh, S.Y., Kang, S.G., Chiu, P.C., 2010. Degradation of 2,4-dinitrotoluene by persulfate activated with zero-valent iron. Sci. Total Environ. 408 (16), 3464–3468.
Oh, W., Lisak, G., Webster, R.D., Liang, Y., Veksha, A., Giannis, A., Moo, J.G.S., Lim, J., Lim, T., 2018. Insights into the thermolytic transformation of lignocellulosic biomass waste to redox-active carbocatalyst: durability of surface active sites. Appl. Catal. B Environ. 233, 120–129.
Oh, W.D., Dong, Z.L., Lim, T.T., 2016. Generation of sulfate radical through heterogeneous catalysis for organic contaminants removal: current development, challenges and prospects. Appl. Catal. B Environ. 194, 169–201.
Peluffo, M., Pardo, F., Santos, A., Romero, A., 2016. Use of different kinds of persulfate activation with iron for the remediation of a PAH-contaminated soil. Sci. Total Environ. 563, 649–656.
Rummel, C.D., Jahnke, A., Gorokhova, E., Kühnel, D., Schmitt-Jansen, M., 2017. Impacts of biofilm formation on the fate and potential effects of microplastic in the aquatic environment. Environ. Sci. Technol. Lett. 4 (7), 258–267.
Shao, P., Tian, J., Yang, F., Duan, X., Gao, S., Shi, W., Luo, X., Cui, F., Luo, S., Wang, S., 2018. Identification and regulation of active sites on nanodiamonds: establishing a highly efficient catalytic system for oxidation of organic contaminants.

Adv. Funct. Mater. 28 (13), 1705295.
Shen, M., Zeng, G., Zhang, Y., Wen, X., Song, B., Tang, W., 2019a. Can biotechnology strategies effectively manage environmental (micro)plastics? Sci. Total Environ. 697, 134200.
Shen, M., Zhang, Y., Zhu, Y., Song, B., Zeng, G., Hu, D., Wen, X., Ren, X., 2019b. Recent advances in toxicological research of nanoplastics in the environment: a review. Environ. Pollut. 252 (Pt A), 511–521.
Shen, M., Zhu, Y., Zhang, Y., Zeng, G., Wen, X., Yi, H., Ye, S., Ren, X., Song, B., 2019c. Micro(nano)plastics: unignorable vectors for organisms. Mar. Pollut. Bull. 139, 328–331.
Song, B., Chen, M., Ye, S.J., Xu, P., Zeng, G.M., Gong, J.L., Li, J., Zhang, P., Cao, W.C., 2019a. Effects of multi-walled carbon nanotubes on metabolic function of the microbial community in riverine sediment contaminated with phenanthrene. Carbon 144, 1–7.
Song, B., Zeng, Z.T., Zeng, G.M., Gong, J.L., Xiao, R., Ye, S.J., Chen, M., Lai, C., Xu, P., Tang, X., 2019b. Powerful combination of g-C3N4 and LDHs for enhanced photocatalytic performance: a review of strategy, synthesis, and applications. Adv. Colloid Interface Sci. 271 (101999), 1–17.
Tan, X., Liu, Y., Zeng, G., Wang, X., Hu, X., Gu, Y., Yang, Z., 2015. Application of biochar for the removal of pollutants from aqueous solutions. Chemosphere 125, 70–85.
Tanaka, K., Takada, H., Yamashita, R., Mizukawa, K., Fukuwaka, M.A., Watanuki, Y., 2013. Accumulation of plastic-derived chemicals in tissues of seabirds ingesting marine plastics. Mar. Pollut. Bull. 69 (1–2), 219–222.
Tang, L., Liu, Y., Wang, J., Zeng, G., Deng, Y., Dong, H., Feng, H., Wang, J., Peng, B., 2018. Enhanced activation process of persulfate by mesoporous carbon for degradation of aqueous organic pollutants: electron transfer mechanism. Appl. Catal. B Environ. 231, 1–10.
Taylor, M.L., Gwinnett, C., Robinson, L.F., Woodall, L.C., 2016. Plastic microfibre ingestion by deep-sea organisms. Sci. Rep. 6, 33997.
Turner, A., Holmes, L.A., 2015. Adsorption of trace metals by microplastic pellets in fresh water. Environ. Chem. 12 (5), 600.
Wang, H., Zeng, Z., Xu, P., Li, L., Zeng, G., Xiao, R., Tang, Z., Huang, D., Tang, L., Lai, C., Jiang, D., Liu, Y., Yi, H., Qin, L., Ye, S., Ren, X., Tang, W., 2019a. Recent progress in covalent organic framework thin films: fabrications, applications and perspectives. Chem. Soc. Rev. 48 (2), 488–516.
Wang, W.J., Zeng, Z.T., Zeng, G.M., Zhang, C., Xiao, R., Zhou, C.Y., Xiong, W.P., Yang, Y., Lei, L., Liu, Y., Huang, D.L., Cheng, M., Yang, Y.Y., Fu, Y.K., Luo, H.Z., Zhou, Y., 2019b. Sulfur doped carbon quantum dots loaded hollow tubular g-C3N4 as novel photocatalyst for destruction of Escherichia coli and tetracycline degradation under visible light. Chem. Eng. J. 378, 122–132.
Wright, S.L., Thompson, R.C., Galloway, T.S., 2013. The physical impacts of microplastics on marine organisms: a review. Environ. Pollut. 178, 483–492.
Wu, P., Cai, Z., Jin, H., Tang, Y., 2019. Adsorption mechanisms of five bisphenol analogues on PVC microplastics. Sci. Total Environ. 650, 671–678.
Xiong, W.P., Zeng, Z.T., Li, X., Zeng, G.M., Xiao, R., Yang, Z.H., Zhou, Y.Y., Zhang, C., Cheng, M., Hu, L., Zhou, C.Y., Qin, L., Xu, R., Zhang, Y.R., 2018. Multiulti-walled carbon nanotube/aminomino-functionalized -53 (Fe)composites: remarkabl adsorptive removal of antibiotics from aqueous solutions. Chemosphere 210, 1061–1069.
Xu, B., Liu, F., Brookes, P.C., Xu, J., 2018. Microplastics play a minor role in tetracycline sorption in the presence of dissolved organic matter. Environ. Pollut. 240, 87–94.
Xu, P., Zeng, G.M., Huang, D.L., Feng, C.L., Hu, S., Zhao, M.H., Lai, C., Wei, Z., Huang, C., Xie, G.X., Liu, Z.F., 2012. Use of iron oxide nanomaterials in wastewater treatment: a review. Sci. Total Environ. 424, 1–10.
Yang, Y., Zhang, C., Lai, C., Zeng, G., Huang, D., Cheng, M., Wang, J., Chen, F., Zhou, C., Xiong, W., 2018. BiOX (X=Cl, Br, I) photocatalytic nanomaterials: applications for fuels and environmental management. Adv. Colloid Interface Sci. 254, 76–93.
Ye, S., Zeng, G., Wu, H., Zhang, C., Dai, J., Liang, J., Yu, J., Ren, X., Yi, H., Cheng, M., Zhang, C., 2017a. Biological technologies for the remediation of co-contaminated soil. Crit. Rev. Biotechnol. 37 (8), 1062–1076.
Ye, S.J., Yan, M., Tan, X.F., Liang, J., Zeng, G.M., Wu, H.P., Song, B., Zhou, C.Y., Yang, Y., Wang, H., 2019a. Facile assembled biochar-based nanocomposite with improved graphitization for efficient photocatalytic activity driven by visible light. Appl. Catal. B Environ. 250, 78–88.
Ye, S.J., Zeng, G.M., Tan, X.F., Wu, H.P., Liang, J., Song, B., Tang, N., Zhang, P., Yang, Y.Y., Chen, Q., 2020. Nitrogen-doped biochar fiber with graphitization from Boehmeria nivea for promoted peroxymonosulfate activation and non-radical degradation pathways with enhancing electron transfer. Appl. Catal. B Environ. 269 (118850), 1–11.
Ye, S.J., Zeng, G.M., Wu, H.P., Liang, J., Zhang, C., Dai, J., Xiong, W.P., Song, B., Wu, S.H., Yu, J.F., 2019b. The effects of activated biochar addition on remediation efficiency of co-composting with contaminated wetland soil. Resour. Conserv. Recycl. 140, 278–285.
Ye, S.J., Zeng, G.M., Wu, H.P., Zhang, C., Liang, J., Dai, J., Liu, Z.F., Xiong, W.P., Wan, J., Xu, P.A., Cheng, M., 2017b. Co-occurrence and interactions of pollutants, and their impacts on soil remediation-A review. Crit. Rev. Environ. Sci. Technol. 47 (16), 1528–1553.
Yi, H., Yan, M., Huang, D.L., Zeng, G.M., Lai, C., Li, M.F., Huo, X.Q., Qin, L., Liu, S.Y., Liu, X.G., Li, B.S., Wang, H., Shen, M.C., Fu, Y.K., Guo, X.Y., 2019. Synergistic effect of artificial enzyme and 2D nano-structured Bi2WO6 for eco-friendly and efficient biomimetic photocatalysis. Appl. Catal. B Environ. 250, 52–62.
Yu, J., Tang, L., Pang, Y., Zeng, G., Wang, J., Deng, Y., Liu, Y., Feng, H., Chen, S., Ren, X., 2019. Magnetic nitrogen-doped sludge-derived biochar catalysts for persulfate activation: internal electron transfer mechanism. Chem. Eng. J. 364, 146–159.
Zeng, Z., Ye, S., Wu, H., Xiao, R., Zeng, G., Liang, J., Zhang, C., Yu, J., Fang, Y., Song, B., 2019. Research on the sustainable efficacy of g-MoS2 decorated biochar nanocomposites for removing tetracycline hydrochloride from antibiotic-polluted aqueous solution. Sci. Total Environ. 648, 206–217.
Zhang, H., Wang, J., Zhou, B., Zhou, Y., Dai, Z., Zhou, Q., Chriestie, P., Luo, Y., 2018a. Enhanced adsorption of oxytetracycline to weathered microplastic polystyrene: kinetics, isotherms and influencing factors. Environ. Pollut. 243 (Pt B), 1550–1557.
Zhang, L.H., Zhang, J.C., Zeng, G.M., Dong, H.R., Chen, Y.N., Huang, C., Zhu, Y., Xu, R., Cheng, Y.J., Hou, K.J., Cao, W.C., Fang, W., 2018b. Multivariate relationships between microbial communities and environmental variables during co-composting of sewage sludge and agricultural waste in the presence of PVP-AgNPs. Bioresour. Technol. 261, 10–18.
Zhang, P., Tan, X.F., Liu, S.B., Liu, Y.G., Zeng, G.M., Ye, S.J., Yin, Z.H., Hu, X.J., Liu, N., 2019. Catalytic degradation of estrogen by persulfate activated with iron-doped graphitic biochar: process variables effects and matrix effects. Chem. Eng. J. 378, 122–141.
Zhang, X., Wang, H., He, L., Lu, K., Sarmah, A., Li, J., Bolan, N.S., Pei, J., Huang, H., 2013. Using biochar for remediation of soils contaminated with heavy metals and organic pollutants. Environ. Sci. Pollut. Res. 20 (12), 8472–8483.
Zhou, C., Zeng, Z., Zeng, G., Huang, d., Xiao, R., Cheng, M., Zhang, C., Xiong, W., Lai, C., Yang, Y., Wang, W., Yi, H., Li, B., 2019. Visible-light-driven photocatalytic degradation of sulfamethazine by surface engineering of carbon nitride:Properties, degradation pathway and mechanisms. J. Hazard Mater. 380, 120815.
Zhu, K., Jia, H., Zhao, S., Xia, T., Guo, X., Wang, T., Zhu, L., 2019. formation of environmentally persistent free radicals on microplastics under light irradiation. Environ. Sci. Technol. 53 (14), 8177–8186.
Zhu, S., Huang, X., Ma, F., Wang, L., Duan, X., Wang, S., 2018. Catalytic removal of aqueous contaminants on N-doped graphitic biochars: inherent roles of adsorption and nonradical mechanisms. Environ. Sci. Technol. 52 (15), 8649–8658.